# A Comprehensive Analysis in Terms of Molecule-Intrinsic, Quasi-Atomic Orbitals. III. The Covalent Bonding Structure of Urea

Aaron C. West, Michael W. Schmidt, Mark S. Gordon, and Klaus Ruedenberg*

Department of Chemistry and Ames Laboratory USDOE, Iowa State University, Ames, Iowa 50011, United States

Ⓢ Supporting Information

ABSTRACT: The analysis of molecular electron density matrices in terms of quasi-atomic orbitals, which was developed in previous investigations, is quantitatively exemplified by a detailed application to the urea molecule. The analysis is found to identify strong and weak covalent bonding interactions as well as intramolecular charge transfers. It yields a qualitative as well as quantitative ab initio description of the bonding structure of this molecule, which raises questions regarding some traditional rationalizations.
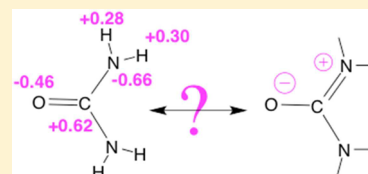
1. INTRODUCTION

In two preceding papers, a rigorous analysis of molecular ab initio wave functions was devised with the aim of transforming their density matrices into sums of contributions that yield intra-atomic energies and interatomic interactions. The resolution is expected to shed light on the qualitative and quantitative synergisms between the various physical interactions that cause bond-forming energy lowerings and, thereby, to provide insights into the bonding patterns of molecules. The first of the preceding papers[1] dealt with Hartree–Fock wave function. In the second paper,[2] the analysis was extended to strongly correlated wave functions.

The present study is the first to test and exemplify the workings of the approach in detail. The method is applied to interpret the bonding pattern that is generated by the electron distribution in urea, $CO(NH_2)_2$. While urea is a nontrivial poly-atomic molecule including carbon, oxygen, nitrogen, and hydrogen atoms, a complete coherent overview of the bonding structure can be attained and displayed because the molecular symmetry limits the amount of unique numerical data. Also, urea is an important molecule in many contexts.

Urea continues to be a subject of current work in basic research areas of chemical physics. The vibrational spectrum has been frequently examined, most recently in an argon matrix isolation environment.[3] By virtue of its unique optical properties, urea plays a role in nonlinear optics research.[4] Among X-ray crystallographers, urea has been of significant interest to those who pursue charge-density refinements.[5] On the other hand, urea is important in biochemical contexts. It is essential for the nitrogen metabolism of proteins by mammals, and it is widely used as a source of nitrogen in fertilizers. Urea is also an important industrial raw material. Friedrich Wöhler's synthesis of urea[6] from silver cyanate and ammonium chloride in 1828 famously marked the beginning of the end of the theory of vitalism in chemistry and the beginning of modern organic chemistry.

The present ab initio analysis furnishes a detailed global picture of the covalent bonding patterns and charge transfers between the atoms. Not only are the primary bonds exhibited, but secondary vicinal bonding effects, i.e., weak conjugation and

hyperconjugation, are also identified. In this context, the kinetic bond orders, which were introduced in the second paper,[2] prove useful because they yield energetic information that is not provided by the density matrix alone.

2. QUASI-ATOMIC ORBITAL ANALYSIS

The urea molecule is displayed in Figure 1. The atoms O, C, N_1, and N_2 lie in a plane. On each N atom, the bonds toward the
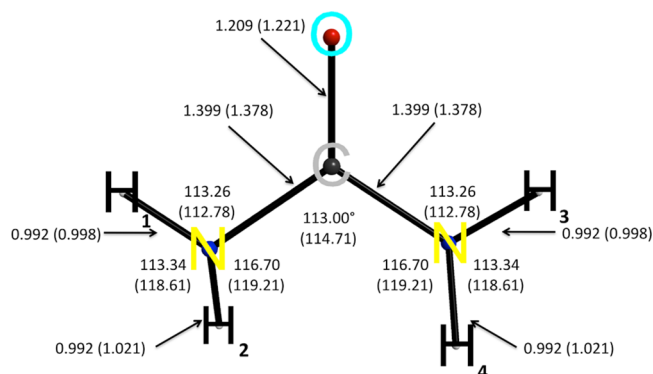
Figure 1. Bond distances (Å) and angles (deg) of urea at the minimum geometry based on the (14,11)CAS wave function using the cc-pVQZ basis. Experimental gas phase values are in parentheses. See ref 7.

two H atoms, the bond toward the C atom, and the lone pair orbital on the N atom form an approximately tetrahedral pattern. The hydrogen atoms are turned in such way that the molecule has C_2 symmetry. Within this symmetry, the atoms H_1 and H_3 are symmetry equivalent, as are the atoms H_2 and H_4. Figure 1 also shows that the theoretical bond distances and angles (without parentheses) that are obtained and used in the present work are close to the experimental values[7] (in parentheses).

2.1. Wave Function. In the conceptual valence orbital space, a reduced complete active space (CAS) multiconfiguration-self-consistent field (MCSCF) wave function was calculated using the occupation restricted multiple active space (ORMAS) design.[8] The valence orbital space is partitioned into the following three groups:

(i) A valence group consisting of five doubly occupied orbitals, namely,

the 2s-type lone pair orbital on O and

the four bonding orbitals between the two N atoms and the respective H atoms.

(ii) A valence group consisting of the following seven orbitals, which are occupied by eight electrons:

the σ-bonding and antibonding orbitals between O and C,

the σ-bonding and antibonding orbitals between C and N_1,

the σ-bonding and antibonding orbitals between C and N_2,

the 2p-type lone-pair orbital on O that lies in the O—C—N_1—N_2 plane (which is found to have a weak hyperconjugative interaction with the σ bonds).

(iii) A valence group consisting of the four $2p\pi$-type orbitals that are perpendicular to the O—C—N_1—N_2 plane, which are occupied by six electrons, viz.: the π-bonding and antibonding orbitals between the C atom and the O atom, as well as the π-lone-pair orbitals on the two N atoms (which are found to interact somewhat with the CO π-bond).

All configurations that satisfy these specifications are included in the wave function. The resulting wave function consists of 28 420 and 14 228 determinants in C_1 and C_2 symmetry, respectively. The analysis of the wave function was performed at the theoretical equilibrium structure according to the procedure outlined previously.[9]

The equilibrium geometry was determined for the described wave function and also for the CAS (14,11) wave function that results from merging the two orbital groups (ii) and (iii) specified above. The equilibrium coordinates of the two calculations differ only in the third decimal places for the bond lengths and in the second decimal places for the bond angles. This good agreement for the geometry supports the presumption that the orbital groups (ii) and (iii) specified above interact very little. The good agreement with the experimental structure is apparent from Figure 1, where theoretical and experimental values are listed. The deviations are similar to those of a previous MP2/6-311++(d,p) calculation.[7]

The calculations were made with the Dunning quadruple-ζ basis sets cc-pVQZ.[10] All calculations were performed with the GAMESS program suite for molecular calculations.[11,12]

2.2. Localized Bonding, Antibonding, and Lone-Pair Orbitals (Split-Localized Orbitals). The bonding and correlation pattern that is created by the described wave function is exhibited by the split-localized valence orbitals, which are displayed in Figure 2. Only the symmetry-unique orbitals are shown. Positive lobes are red; negative lobes are blue. The contour surfaces correspond to absolute orbital values of 0.1 (electron/bohr^3)$^{1/2}$. The contour surfaces for 0.05 (electron/bohr^3)$^{1/2}$ look practically the same. Under the orbital plots, the orbital labels (explained in the subsequent paragraphs) and the orbital occupations (in electron units) are indicated.

The 2s-type lone pair orbital on oxygen, Osl, is doubly occupied by construction. For each of the CO, CN, and NH σ-bonds, there is a bonding and an antibonding orbital, as follows: COσ, COσ*, CNσ, CNσ*, NHσ, and NHσ*. Since the wave function does not contain the NHσ* antibonding orbitals,
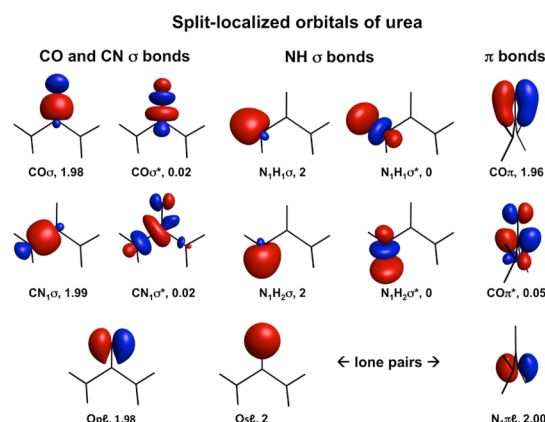
Figure 2. Split-localized orbitals of the ORMAS wave function of urea (see Section 2.2) at the equilibrium geometry. Occupations are next to the orbital symbols, below each orbital. Contour surfaces correspond to 0.1 (electron/bohr^3)$^{1/2}$.

these lowest unoccupied molecular orbitals (LUMOs) were obtained by the valence virtual orbital (VVO) recovery procedure.[13] Although their occupations are zero, they are relevant for the formation of the quasi-atomic orbitals (QUAOs) in the next section.

By construction, the NHσ* antibonding orbitals lie in the VVO space and thus have zero occupations; they are LUMOs. The COσ* and CNσ* antibonding orbitals have occupations of 0.02e, which indicates that they provide some correlation. The occupations of COσ and COσ* add up to a bond population of 2.

But the sum of the occupations of CNσ and CNσ* exceeds 2. The excess population is donated by the 2p-type lone pair orbital Opl on oxygen, which lies in the OCNN plane. It is also apparent that the CNσ* antibonding orbital extends into the region of the Opl orbital. These two observations suggest the existence of a *hyperconjugative vicinal* interaction between the Opl lone pair on oxygen and the orbitals that are localized in the two CN bonds.

The π-molecular orbital Nπl is a doubly occupied lone pair orbital on nitrogen. The bonding orbital COπ and the antibonding orbital COπ* form the CO π-bond. The occupation of 0.05e for COπ* implies a stronger correlation than that found in the CO σ-bonds. The orbital COπ* also extends somewhat toward the nitrogen atoms.

The overall implication of these orbitals and occupations is the bond pattern expressed by the single Lewis structure with a CO double bond and π-lone pairs on the nitrogen atoms. A more detailed bonding picture will be furnished by the analysis in terms of oriented QUAOs.

2.3. Oriented Quasi-Atomic Orbitals and Density Matrix. Figure 3 exhibits the *oriented valence QUAOs* that are obtained from the present wave function.[14] The symbols that label the QUAOs in this figure imply their chemical functions according to the following scheme. Each symbol consists of several parts. The first part is always the atomic symbol of the atom *on which the QUAO is located*.

If the QUAO is a bonding orbital, then the second part of the QUAO symbol is the atomic symbol, *written in lower case font*, of the atom *to which this QUAO establishes a bond*. The third part of the QUAO symbol contains a characterization of the bond type. For instance, Coπ denotes a QUAO on a carbon atom that establishes a π-bond to an oxygen atom. Mgbrσ would denote a QUAO on magnesium establishing a σ-bond to bromine.

If a nonbonded QUAO contains close to two electrons, then the second part of the QUAO symbol characterizes it as a lone pair.

Oriented QUAOs of urea
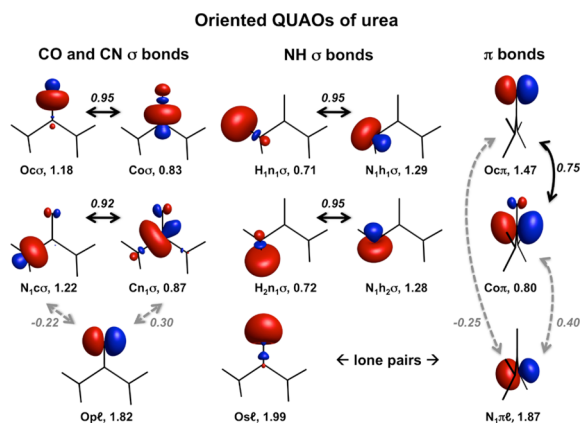
Figure 3. Oriented QUAOs of the ORMAS wave function of urea at the equilibrium geometry. The orbital symbols and the orbital occupations are below each orbital. Strong and weak bonds are indicated by solid black and weak gray arrows, respectively. The bond orders are given next to the respective arrows.

Thus, Csl, Opl, Nπl denote an s-type lone pair on carbon, a p-type on oxygen, and a π-type lone pair on nitrogen, respectively.

If a nonbonded QUAO contains approximately one electron, then the second part of the QUAO symbol characterizes it as a radical. For instance, Opr$d$ would denote a p-type radical QUAO on an oxygen atom.

In Figure 3, only the symmetry-unique QUAOs are shown. The contour surfaces correspond to absolute orbital values of 0.1 (electron/bohr^3)$^{1/2}$. In accordance with the described conventions, the following QUAOs are displayed.

$|Osl\rangle$ = 2s-type hybrid lone pair orbital on O
$|Opl\rangle$ = 2p-type lone pair orbital on O, lying in the plane of the atoms O, C, N$_1$, and N$_2$
$|Oc\pi\rangle$ = 2pπ-type orbital on O, π-bonding to C
$|Oc\sigma\rangle$ = 2pσ-type hybrid orbital on O, σ-bonding to C
$|Co\sigma\rangle$ = 2pσ-type hybrid orbital on C, σ-bonding to O
$|Co\pi\rangle$ = 2pπ-type orbital on C, π-bonding to O
$|Cn_1\sigma\rangle$ = 2pσ-type hybrid orbital on C, σ-bonding to N$_1$
$|Cn_2\sigma\rangle$ = 2pσ-type hybrid orbital on C, σ-bonding to N$_2$
$|N_1c\sigma\rangle$ = 2pσ-type hybrid orbital on N$_1$, σ-bonding to C
$|N_1\pi l\rangle$ = 2pπ-type lone pair orbital on N$_1$
$|N_1h_1\sigma\rangle$ = 2pσ-type hybrid orbital on N$_1$, σ-bonding to H$_1$
$|N_1h_2\sigma\rangle$ = 2pσ-type hybrid orbital on N$_1$, σ-bonding to H$_2$
$|H_1n_1\sigma\rangle$ = 1s-type orbital on H$_1$, σ-bonding to N$_1$
$|H_2n_1\sigma\rangle$ = 1s-type orbital on H$_2$, σ-bonding to N$_1$

In terms of these orthogonal oriented QUAOs, the first-order (spin-averaged) symmetric spatial density matrix has the expansion

$$\rho(1, 2) = \sum_{Aa} \sum_{Bb} p_{Aa,Bb} |Aa(1)\rangle |Bb(2)\rangle \tag{1}$$

where the symbol $|Aa(i)\rangle$ denotes the value of the orbital a on atom A at the spatial position coordinate of electron i. The sums go over all oriented QUAOs in the molecule. The diagonal elements $p_{Aa,Aa}$ are the orbital populations. They are shown under the respective orbitals in Figure 3. The interatomic off-diagonal elements are the bond orders, whose absolute values are intrinsically limited[15] to $0 \leq |p_{Aa,Bb}| \leq 1$. In Figure 3, the strong bonds (i.e., for $p_{Aa,Bb} > 0.5$) are indicated by black arrows, the weaker ones (i.e., for $0.2 < |p_{Aa,Bb}| < 0.5$) by gray arrows. The respective bond order values are shown next to the arrows.

The complete density matrix is listed in Tables S1 and S2 of the Supporting Information. These tables are divided into blocks corresponding to atoms. The columns for O, C, and N$_1$ are listed in Table S1; the columns for N$_1$, H$_1$, H$_2$, N$_2$, H$_3$, and H$_4$ are listed in Table S2. The rows and columns are labeled by the orbital symbols given above. Each strong bond order (i.e., >0.5) is marked by the colors of the two atoms between which the bond is formed. The weak bonds orders ($0.2 < |p_{Aa,Bb}| < 0.5$) are indicated by light blue-green shading. The remaining off-diagonal elements listed in these tables are all ≤0.13. Elements with values less than 0.02 have been suppressed in the tables. The bond orders in these tables are listed with the signs that correspond to the phases of the orbital plots in Figure 3.

Some of the weak bond orders in Figure 3 have negative signs. Nonetheless, the corresponding interactions between the respective QUAOs are bonding. This conclusion is established through the kinetic bond orders that are discussed in the next section.

2.4. Bond Order Analysis. In ab initio wave functions, the essential contributions to covalent bonding come from the kinetic interference energies between atomic orbitals.[16,17] For the orthogonal QUAOs, these energies are simply the products of the "density bond orders" mentioned in the preceding section and the kinetic energy integrals between the corresponding orbitals. The assessment of bonding by means of the density bond orders goes back to Coulson and co-workers.[18,19] In the second paper of this series, we introduced[20] the *kinetic bond orders (KBOs)*, which are scaled kinetic interference energies, as energetic indicators of the bonding strength between quasi-atomic orbitals. The KBO signs are independent of the phases of the QUAOs.

The strong and the moderately weak bonding interactions in urea are collected in Table 1. In addition to the density bond

Table 1. Strong and Weak Bond Orders (BOs $p_{Aa,Bb}$) and Kinetic Bond Orders (KBOs $k_{Aa,Bb}$) between Oriented Valence Quasi-Atomic Orbitals (QUAOs) of Urea

interacting QUAOs	BO $p_{Aa,Bb}$	KBO (kcal/mol) $k_{Aa,Bb}$
Interactions between π QUAOs		
Ocπ−Coπ	0.751	−47.8
Coπ−N$_1\pi l$	0.396	−8.0
Ocπ−N$_1\pi l$	−0.248	−4.9
N$_1\pi l$−N$_2\pi l$	−0.131	−0.5^a
Interactions between Neighboring σ QUAOs		
Coσ−Ocσ	0.954	−94.9
Cn$_1\sigma$−N$_1$cσ	0.919	−58.4
N$_1$h$_2\sigma$−H$_2$n$_1\sigma$	0.950	−43.3
N$_1$h$_1\sigma$−H$_1$n$_1\sigma$	0.946	−42.9
Interactions between Vicinal σ QUAOs		
Cn$_1\sigma$−Opl (Ia)	0.299	−17.9
N$_1$cσ−Opl (Ib)	−0.223	−8.7
N$_1$cσ−N$_2$cσ (IIa)	−0.108	−1.2
N$_1$cσ−Cn$_2\sigma$ (IIb)	0.053	−1.0
N$_1$h$_2\sigma$−Coσ (IIIa)	−0.088	−0.8
Cn$_2\sigma$−N$_1$h$_1\sigma$ (IIIb)	−0.098	−0.6

^{a}Even though this value is less than 0.6 kcal/mol in magnitude, this bond is included here to complete the π system.

orders $p_{Aa,Bb}$, The table also lists the KBOs $k_{Aa,Bb}$. The table contains all symmetry unique pairs of oriented orbitals between which the KBO is 0.6 kcal/mol or larger in magnitude. In addition, one interaction with a KBO = −0.5 kcal/mol is included to complete the π-bonding system. In confirmation of our previous discussions,[16,17] *all KBOs $k_{Aa,Bb}$ are seen to be negative; that is, they*

represent bonding energy contributions, regardless of the phase-dependent signs of the bond orders $p_{Aa,Bb}$. Moreover, these energetic characteristics make sharper distinctions than do the density bond orders between the different bonds. The following discussion of bond strengths is therefore based on the KBO values.

The upper section of Table 1 contains the bond orders between the π-orbitals. It is apparent that only the π-bond between carbon and oxygen is strong. The KBO of each of the CN π-bonds (-8.0 kcal/mol) is less than a sixth of the KBO of the CO π-bond (-47.8 kcal/mol) in magnitude. Correspondingly, the vicinal π-interaction between the two nitrogen atoms (-0.5 kcal/mol) is only $\sim$10% of the vicinal π-interaction between nitrogen and oxygen (-4.9 kcal/mol) in magnitude. The implication is that there is some, but only a slight conjugation between the π-lone pairs on nitrogen and the CO π-bond.

The middle section of Table 1 contains the strong σ-bonds. All bond orders are within 10% of the possible maximum[15] of 1.0. Adding the π and σ KBO of the CO bond contributions together yields the total KBO values of -142.7 kcal/mol. For the CN and NH single σ-bonds one has -58.4 and -42.9 kcal/mol, respectively. The corresponding empirically inferred average bond energies are roughly 125.5, 43.9, and 56.5 kcal/mol.[21] The approximate character of our KBO formulation was commented upon in the preceding paper.[22]

The bottom section in Table 1 exhibits the weak σ-interactions, but with KBO values still $\geq$0.6 kcal/mol in magnitude. All these KBOs represent interactions between *vicinally* positioned oriented QUAOs. The labels listed after the orbital pairs in this section of Table 1 refer to Figure 4, where these interactions are
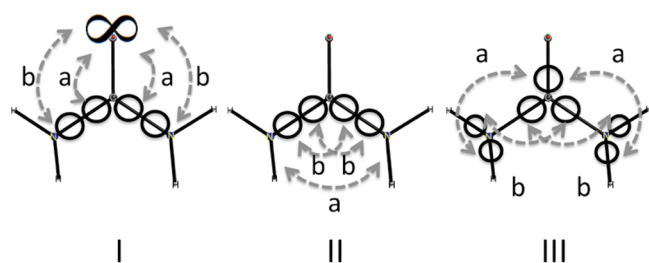
Figure 4. Hyperconjugative interactions between vicinal QUAOs. Every circle represents one σ-bonding QUAO. The figure 8 at the top of the figure represents the Opl QUAO on oxygen. The Roman numerals and labels a,b are referred to in Table 1.

schematically indicated. The most important of them (Ia,Ib) are between Opl, the lone pair on oxygen that lies in the OCNN plane, and the orbitals that form the CN bonds. These interactions manifestly represent *hyperconjugative interactions* in the σ-bonding system. Remarkably, the KBO values of -17.9 and -8.7 kcal/mol imply that these interactions are in fact stronger than the weak conjugation between the π-orbitals on the N atoms and the π-orbitals in the CO bond discussed above, which have KBO values of -4.9 and -0.5 kcal/mol. The last four interactions in this table are an order of magnitude smaller, barely above 0.6 kcal/mol. They are between σ-type QUAOs on carbon and nitrogen, as also indicated in Figure 4.

All remaining interactions between pairs of oriented QUAOs have KBOs of less than 0.6 kcal/mol in magnitude. Table 2 contains a list of all of QUAO pairs that have KBOs larger than 0.1 kcal/mol in magnitude. All remaining interactions between QUAO pairs are even weaker.

It is a significant vindication of the KBO concept that all strong and weak interatomic KBOs in Table 1 *as well as the very weak*

Table 2. Bond Orders (BOs $p_{Aa,Bb}$) and Kinetic Bond Orders (KBOs $k_{Aa,Bb}$) between Oriented Valence QUAOs of Urea, for which 0.1 kcal/mol < |$k_{Aa,Bb}$|< 0.6 kcal/mol

interacting QUAOs	BO $p_{Aa,Bb}$	KBO (kcal/mol) $k_{Aa,Bb}$
Cn$_1\sigma$–Cn$_2\sigma$	0.023	0.6
H$_3$n$_2\sigma$–N$_1$cσ	0.105	-0.4
Coσ–Cn$_1\sigma$	-0.026	-0.4
H$_2$n$_1\sigma$–Cn$_1\sigma$	0.036	-0.4
N$_1$h$_1\sigma$–Coσ	0.037	-0.4
N$_1$h$_2\sigma$–Coπ	-0.054	-0.4
H$_1$n$_1\sigma$–Cn$_1\sigma$	0.035	-0.4
H$_2$n$_1\sigma$–H$_1$n$_1\sigma$	0.031	-0.4
N$_1$h$_2\sigma$–N$_1$h$_1\sigma$	-0.026	-0.4
N$_1$h$_2\sigma$–Opl	-0.044	-0.3
N$_1$cσ–N$_1$h$_2\sigma$	-0.021	-0.3
H$_2$n$_1\sigma$–Ocσ	0.078	-0.3
N$_1$h$_1\sigma$–Opl	-0.048	-0.3
H$_2$n$_1\sigma$–Opl	0.058	-0.3
N$_1$cσ–Ocσ	0.025	-0.3
N$_1$h$_2\sigma$–Cn$_2\sigma$	0.018	-0.3
N$_1$cσ–N$_1$h$_1\sigma$	-0.013	-0.3
Cn$_1\sigma$–Osl	-0.044	0.2
H$_2$n$_1\sigma$–Ocπ	0.057	-0.2
N$_1$cσ–N$_2$h$_4\sigma$	-0.026	-0.2
H$_1$n$_1\sigma$–Osl	0.037	-0.2
N$_1$h$_1\sigma$–N$_2$h$_3\sigma$	0.031	-0.1
Ocσ–Osl	0.011	0.1
N$_1$h$_1\sigma$–Osl	-0.029	-0.1
N$_1$h$_2\sigma$–N$_1\pi l$	0.024	0.1
N$_1$h$_1\sigma$–Ocσ	-0.028	-0.1
N$_1\pi l$–N$_2$h$_4\sigma$	-0.035	-0.1
N$_1$h$_2\sigma$–Ocσ	0.024	-0.1
N$_1$h$_1\sigma$–N$_1\pi l$	0.013	0.1

interatomic KBOs in Table 2 are negative, i.e., bonding, with the single exception of the very small (0.2 kcal/mol) KBO between the QUAOs Osl and Cn$_1\sigma$. This observation lends support to considering the KBOs as indicative of the strengths of bonding interactions.

2.5. Population Analysis. The occupations of the oriented valence QUAOs for the symmetry unique atoms are collected in Table 3. The *rows* correspond to atoms, with the total atomic valence populations Q_A listed in the first column. The orbitals placed in any one *column* are the orbitals from different atoms between which bonding interactions exist as deduced from the preceding bond order analysis. The last row for each column shows the total number of electrons involved in that bonding group. The slight deviations from integer numbers are due to the use of *unrestrained* QUAOs.[23]

The second column in Table 3 contains only the 2s-type lone pair orbital on oxygen. Its occupation of 1.99e implies that it is nonbonding. The third column (OCNπ) displays the occupations of the π-orbitals. The total occupation is very close to six electrons, which corresponds to the reference model that Ocπ, Coπ, N$_1\pi l$, and N$_2\pi l$ originally have the occupations 1, 1, 2, and 2, respectively. With respect to this original distribution, there is a charge shift of $\sim$0.47e into the oxygen π-orbital, of which $\sim$0.20e comes from carbon and 0.135e comes from each nitrogen.

The fourth column (OCσ) in Table 3 lists the occupations of the two orbitals that form the CO-σ bond. The total occupation

Table 3. Atomic Valence Populations, Quasi-Atomic Orbital Occupations, and Bond Populations of the Oriented Valence Quasi-Atomic Orbitals of Urea[a]

atoms	QA[b]		groups of bonded orbitals				
			$OCN\pi$	$OC\sigma$	$NCO\sigma$	$N_1H_1\sigma$	$N_1H_2\sigma$
O		Osl	$Oc\pi$	$Oc\sigma$	Opl		
	6.460	1.990	1.471	1.183	1.816		
C			$Co\pi$	$Co\sigma$	$Cn_1\sigma$		
	3.374[c]		0.801	0.833	0.870		
N_1			$N_1\pi l$		$N_1c\sigma$	$N_1h_1\sigma$	$N_1h_2\sigma$
	5.661		1.865		1.221	1.281	1.294
H_1	0.717					$H_1n_1\sigma$	
						0.717	
H_2	0.705						$H_2n_1\sigma$
							0.705
QB[d]	24	1.990	6.002[e]	2.016	5.998[f]	1.998	1.999

[a]Only symmetry unique atoms are shown. [b]Atomic populations. [c]Includes the $Cn_2\sigma$ orbital in addition to the exhibited orbitals $Co\sigma$, $Co\pi$, and $Cn_1\sigma$. [d]Sum of populations in each column. [e]Includes $N_2\pi l$ orbital in addition to the listed orbitals $Oc\pi$, $Co\pi$, and $N_1\pi l$. [f]Includes the orbitals $Cn_2\sigma$ and $N_2c\sigma$ in addition to the listed orbitals Opl, $Cn_1\sigma$, and $N_1c\sigma$.

is close to 2e, with a charge shift of 0.183e from carbon to oxygen. The situation is similar for the NH bonds, listed in the sixth and seventh column. Each bond has a total population of ~2e with a charge shifts of ~0.28e and ~0.30e from the hydrogens to the nitrogen.

The fifth column ($NCO\sigma$) shows the orbitals that establish the CN_1 σ-bond as well as the Opl lone pair orbital on O that lies in the plane of the atoms O, C, N_1, and N_2. The $N_1c\sigma$ orbital gains ~0.22e, of which 0.13e comes from the $Cn_1\sigma$ orbital and ~0.09e comes from the Opl orbital. The same holds of course for $N_2c\sigma$, $Cn_2\sigma$, and Opl. The charge transfer from Opl, which lowers the double occupancy of Opl, generates the electron sharing that establishes the hyperconjugative vicinal bonding interactions between the Opl orbital and the $N_1c\sigma$ orbital, which the analysis of the bond orders had already indicated. The analogous hyperconjugative charge transfer occurs between Opl and $N_2c\sigma$. The total number of electrons in these five orbitals is close to six.

3. THE GLOBAL BONDING STRUCTURE

The quasi-atomic analysis procedure generates a global analysis of the bonding, nonbonding, and antibonding interactions in a molecule by means of a rigorous resolution of the ab initio wave function and its energy. The present study exemplifies the method by applying it to a strongly correlated wave function of urea, which closely reproduces the molecular geometry.[24] The QUAOs, the orbital populations, and the density bond orders that result from this approach are documented. The design of the full energy decomposition analysis on this basis is in progress. Those parts of this energy analysis that contain the essential interactions responsible for creating bonds are included in the present study as the KBOs.

3.1. Ab Initio Elements of the Bonding Structure. The following elements of the bonding pattern emerge from the global density matrix analysis.

(i) The principal structure is that of a $\sigma + \pi$ double bond between carbon and oxygen (KBO sum −142.7 kcal/mol); all other bonds are essentially single bonds (with KBOs of −42.9 to −94.1 kcal/mol).

(ii) A weak conjugation exists between the CO π-bond and the π-lone pairs on the two nitrogen atoms (with KBOs of −4.9 to −8.0 kcal/mol).

(iii) Furthermore, hyperconjugative interactions exist between the in-plane 2p-type lone pair on oxygen and the two vicinal CN σ-bonds (with KBOs of ca. −8.7 to −17.9 kcal/mol). According to the KBO values in Table 1, the total of the hyperconjugative interactions in the σ-system is about twice as strong as the total of the weak CN π-conjugations.

Within the context of this bonding structure, strong charge shifts occur. From the total atomic valence populations in Table 3, it follows that there is a *total* charge transfer of ~0.46e to the oxygen atom and ~0.66e to each nitrogen atom. The carbon atom loses ~0.62e. Two of the hydrogens lose ~0.28e, and two lose ~0.30e.

These totals can be resolved into charge flows between individual QUAOs by assuming the following electron distribution "before charge transfer": Each σ-bonded oriented QUAO has exactly one electron, and the same holds for the oxygen and carbon π-orbitals that form the π-bond. On the other hand, the lone pair orbitals Osl and Opl on oxygen as well as the π-type lone pair on each nitrogen all have exactly two electrons. With these before-transfer reference populations, the charge transfers for the individual QUAOs can be deduced from Table 3.

Furthermore, these charge transfers to and from the individual QUAOs can be related to the discussed bonding information because the conjugation in the π-system and the hyperconjugation between the Opl orbital on oxygen and the CN σ-bonds *are contingent upon partial electron donation from the doubly occupied Opl and $N\pi l$ orbitals to share electrons with those orbitals to which they are weakly bonded.*

From this analysis, the global bonding structure between all 20 QUAOs emerges that is schematically displayed in Figure 5. The upper part of the figure depicts the σ-system; the lower part depicts the π-system. The QUAOs belonging to one atom are placed in a box. Arrows connect the individual QUAOs that are strongly or weakly bonded. The directions of the arrows indicate the directions of the charge transfer. The amount of charge transfer is listed next to each arrow in blue font. The KBO of the bond is shown in red font.

This breakdown implies that the transfer to the oxygen atom (0.46e) occurs almost entirely in the π-system because, in the σ-system, the gain from the carbon atom is essentially canceled by the loss to the two nitrogen atoms. On the other hand, 90% of the charge transfer to each nitrogen atom (~0.66e) comes from
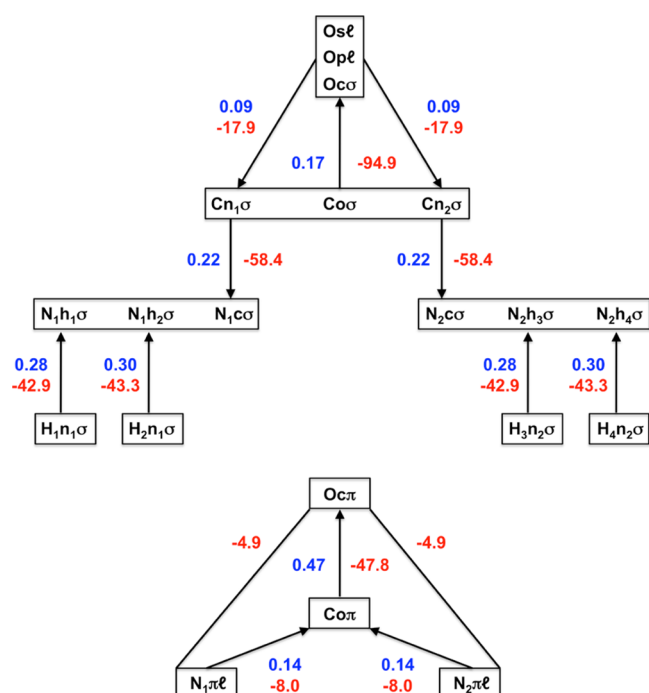
Figure 5. Schematic representation of the pattern of covalent bonding between the quasi-atomic orbitals in urea. The upper figure depicts the σ-system. The lower figure depicts the π-system. Orbitals belonging to the same atom are enclosed in one box. Arrows indicate the bonding and the direction of charge transfers between individual QUAOs. Charge transfers (in electron units) are blue. KBOs (in kcal/mol) are red. In addition to the shown KBOs, there are also KBOs of −8.7 kcal/mol between $Op\ell$ and $N_1c\sigma$ and $N_2c\sigma$.

the hydrogen atoms. Of the electron loss of the carbon atom (∼0.62e), 58% goes to the oxygen atom, and 21% goes to each nitrogen atom.

It is apparent that two kinds of charge transfer occur. In all strong bonds, the charge transfers ($C\sigma{\rightarrow}O\sigma$, $C\sigma{\rightarrow}N\sigma$, $H\sigma{\rightarrow}N\sigma$, and $C\pi{\rightarrow}O\pi$) are associated with the polarization of the electron exchange due to electronegativity differences. In the π-conjugation ($N\pi{\rightarrow}C\pi$) and in the σ-hyperconjugation ($Op\ell \rightarrow$ vicinal $CN\sigma$), the charge transfer is due to electron donation from the lone pair to establish the secondary bonds.

3.2. Inadequacy of the Ionic Resonance Structure. The just discussed bonding structure should be compared to the frequently seen description by the resonance pattern. The aim of
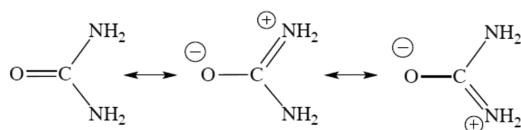
this resonance pattern is to describe the extension of the CO π-bonding to include the π-orbitals on the nitrogen atoms. The main motivation for postulating this π-orbital conjugation is to account for the stability of the planar conformation of the atoms O, C, N, and N and the comparative shortening of the CN bonds.

Relevant to this discussion is the remarkably large charge depletion on the carbon atom and the large charge accumulations at the nitrogen atoms found in the present analysis. These charge displacements were confirmed by the following other approaches for deducing atomic charges:

- The Natural Atomic Orbital (NAO) populations of the Natural Population Analysis (NPA) of Weinhold and co-workers,[25,26] calculated with the NBO6.0 program.[27] The density matrix was obtained from a PBE0 density functional[28] calculation (using GAMESS[11,12]), with the cc-pVQZ basis and at the geometry discussed in Section 2.1.
- The Potential Determined Charges (PDC) of Spackman,[29] calculated by GAMESS[11,12] for the wave function of the present paper discussed in Section 2.1. This method determines the various atomic charge accumulations and depletions by closely fitting their (point charge) electrostatic potential to the *actual* electrostatic potential of the molecule (i.e., of nuclei + electrons) in a large part of the *van der Waals region*.
- The AIM charges of Bader[30,31] for the density of a RHF/6-31G(d,p) calculation of the molecule as reported by C. Gatti et al.[32]
- The AIM charges of Bader[30,31] calculated for an *experimental* density of the urea crystal that was obtained from X-ray diffraction data fitting.[4,33]

All of these approaches agree in yielding a substantial electronic charge depletion on the carbon atom and substantial charge accumulations on the nitrogen atoms and on the oxygen atom, as shown by the following collection of the deduced atomic charges (nuclei + electrons):

Method	QUAO	NAO	PDC	AIM(the)	AIM(exp)
oxygen	−0.46	−0.62	−0.55	−1.44	−1.18
carbon	+0.62	+0.75	+0.91	+2.54	+1.67
nitrogen	−0.66	−0.84	−0.97	−1.47	−1.21
hydrogen1	+0.28	+0.39	+0.39	+0.48	+0.48
hydrogen2	+0.30	+0.38	+0.40	+0.44	+0.49

The differences between the various methods are well within the limits that are to be expected not only by virtue of the different physical aspects that are taken into account by the different definitions, and in view of the different wave functions, basis sets, and optimized geometries. The fact that, these methodological differences notwithstanding, there is a consensus regarding the pronounced relative charge accumulations and depletions on the various atoms represents strong evidence for the physical reality of the implied charge shifts.

Another aspect of the large charge shifts inside the molecule is that urea is calculated to have large quadrupole moments, the largest component being ∼6 Buckingham. (Experimental values do not seem to be available.) The quadrupole components calculated from the fractional point charges listed above differ from the respective *actual* quadrupole components as follows:

Quadrupole values	QUAO	NAO	PDC
average deviation	23%	19%	9%
maximal deviation	36%	48%	20%

These results support the inference of large relative interatomic charge displacements.

These actual charge displacements contradict the charge displacements that are implied by the above-shown resonance pattern. The resonance picture implies (i) an overall positive charge on N, (ii) a small overall negative charge on O, and (iii) a neutral carbon atom. All of these implications are in marked conflict with the values deduced from the ab initio wave function and, indeed, from experiment.

The partial π-conjugation including the nitrogen atoms exists also in the present analysis (KBO ≈ 12.9 kcal/mol in each CN bond), as discussed in the preceding Section 3.1. The existence of this conjugation does not prove the proposed resonance pattern.

3.3. Ab Initio Interpretation of the Bonding Pattern.

The ab initio analysis suggests the following physical bonding interpretation in addition to the basic single bonds and the CO double bond.

In the π-system, the CO π-bond is highly polarized toward the oxygen atom due to the electronegativity difference. The resulting large charge depletion in the carbon π-orbital makes room for some charge donation from the nitrogen π-lone pairs to the carbon π-orbital, which establishes the electron sharing that is the basis for the π-bonding interaction between the carbon and nitrogen π-orbitals.

In the σ-system, on the other hand, σ-bond polarizations from carbon to nitrogen create a σ-charge depletion on carbon, which makes room for electron donation from the in-plane p-lone pair on oxygen to the vicinal CN σ-bond orbitals. This electron sharing creates the hyperconjugation in the σ-system. Note that the hyperconjugation also occurs for the Hartree−Fock wave function, where the antibonding LUMOs are not occupied.

In both cases, the conjugative π-system extension and the *hyperconjugation* in the σ-system, the simultaneous polarization and charge donation are expected to reinforce each other. Both of these weak bonding effects favor the planar arrangement of oxygen, carbon, and the two nitrogen atoms.

The large charge accumulations on the nitrogen atoms result from the polarization of the NH bonds.

■ ASSOCIATED CONTENT

ⓢ Supporting Information

The Supporting Information is available free of charge on the ACS Publications website at DOI: 10.1021/acs.jpca.5b03400.

First-order density matrix of the urea molecule. (PDF)

■ AUTHOR INFORMATION

Corresponding Author
*Phone: 515-294-5253. E-mail: ruedenberg@iastate.edu.

Notes
The authors declare no competing financial interest.

■ ACKNOWLEDGMENTS

■ REFERENCES

(1) West, A. C.; Schmidt, M. W.; Gordon, M. S.; Ruedenberg, K. A Comprehensive Analysis of Molecule-intrinsic Quasi-atomic, Bonding, and Correlating Orbitals. I. Hartree-Fock Wave Functions. *J. Chem. Phys.* **2013**, *139*, 234107 hereafter referred to as Paper I.

(2) West, A. C.; Schmidt, M. W.; Gordon, M. S.; Ruedenberg, K. A Comprehensive Analysis of Molecule-intrinsic, Quasi-atomic Orbitals. II. Strongly Correlated MCSCF Wave Functions. accepted by *J. Phys. Chem. A* **2015**, 150916123848008; hereafter referred to as Paper II.10.1021/acs.jpca.5b03399

(3) Dobrowolski, J. Cz.; Kolos, R.; Sadlej, J.; Mazurek, A. P. Theoretical and IR-matrix Isolation Studies on the Urea and Urea-D_4, -^{13}C, and −1,3-^{15}N$_2$ Substituted Molecules. *Vib. Spectrosc.* **2002**, *29*, 261−282.

(4) Hermet, P.; Ghosez, Ph. First-principles Study of the Dynamical and Nonlinear Optical Properties of Urea Single Crystals. *Phys. Chem. Chem. Phys.* **2010**, *12*, 835−843.

(5) Birkedal, H.; Madsen, D.; Mathiesen, R. H.; Knudsen, K.; Weber, H. P.; Pattison, P.; Schwarzenbach, D. The Charge Density of Urea from Synchrotron Diffraction Data. *Acta Crystallogr., Sect. A: Found. Crystallogr.* **2004**, *A60*, 371−381.

(6) Wöhler, F. Über Künstliche Bildung des Harnstoffs (On the Artificial Formation of Urea). *Ann. Phys.* **1828**, *88*, 253−256.

(7) Godfrey, P. D.; Brown, R. D.; Hunter, A. N. The Shape of Urea. *J. Mol. Struct.* **1997**, *413-414*, 405−414.

(8) See Section 4.2.1 of ref 2.

(9) See Section 4.3 of ref 2.

(10) Dunning, T. H., Jr. Gaussian Basis Sets for use in Correlated Molecular Calculations. I. The atoms Boron through Neon and Hydrogen. *J. Chem. Phys.* **1989**, *90*, 1007−1023.

(11) Schmidt, M. W.; Baldridge, K. K.; Boatz, J. A.; Elbert, S. T.; Gordon, M. S.; Jensen, J. H.; Koseki, S.; Matsunaga, N.; Nguyen, K. A.; Su, S.; et al. General Atomic and Molecular Electronic Structure System. *J. Comput. Chem.* **1993**, *14*, 1347−1363.

(12) Gordon, M. S.; Schmidt, M. W. In *Theory and Applications of Computational Chemistry, the first forty years*; Dykstra, C. E., Frenking, G., Kim, K.S., Scuseria, G. E., Eds.; Elsevier: Amsterdam, 2005; pp 1167−1189.

(13) This recovery is a basic achievement of the present approach. It is described in ref 1 (Section V.A.1) for HF wave functions and in ref 2 (Section 4.3) for MCSCF wave functions.

(14) See Sections 4.2.2 and 4.3 of ref 2.

(15) Ivanic, G.; Atchity, G. J.; Ruedenberg, K. Intrinsic Local Constituents of Molecular Electronic Wave Functions. I. Exact Representation of the Density Matrix in Terms of Chemically Deformed and Oriented Atomic Minimal Basis Set Orbitals. *Theor. Chem. Acc.* **2008**, *120*, 281−294.

(16) Schmidt, M. W.; Ivanic, J.; Ruedenberg, K. Covalent Bonds are Created by the Drive of Electron Waves to Lower their Kinetic Energy through Expansion. *J. Chem. Phys.* **2014**, *140*, 204104.

(17) Schmidt, M. W.; Ivanic, J.; Ruedenberg, K. The Physical Origin of Covalent Bonding. In *The Chemical Bond, Fundamental Aspects of Chemical Bonding*; Frenking, G., Shaik, S., Eds.; Wiley-VCH: Weinheim, Germany, 2014; pp 1−67.

(18) Coulson, C. A.; Longuet-Higgins, H. C. The Electronic Structure of Conjugated Systems. I. General Theory. *Proc. R. Soc. London, Ser. A* **1947**, *191*, 39−60.

(19) Chirgwin, B. H. Summation Convention and the Density Matrix in Quantum Theory. *Phys. Rev.* **1957**, *107*, 1013−1025.

(20) See Section 3.3 of ref 2.

(21) See, for instance, Huheey, J. E.; Keiter, E. A.; Keiter, R. L. *Inorganic Chemistry, Principles of Structure and Reactivity*; Harper Collins: New York, 1993.

(22) See Section 3.3 of ref 2.

(23) See Section 4.2.2 of ref 2.

(24) See the next to the last paragraph of Section 2.1.

(25) Reed, A. E.; Weinstock, R. B.; Weinhold, F. Natural Population Analysis. *J. Chem. Phys.* **1985**, *83*, 735−746.

(26) Landis, C. R.; Weinhold, F. The NBO View of Chemical Bonding. In *The Chemical Bond, Fundamental Aspects of Chemical Bonding*; Frenking, G., Shaik, S., Eds.; Wiley-VCH: Weinheim, Germany, 2014; pp 91−120.

(27) Glendening, E. D.; Landis, C. R.; Weinhold, F. NBO 6.0: Natural Bond Orbital Analysis Program. *J. Comput. Chem.* **2013**, *34*, 1429−1437.

(28) Adamo, C.; Barone, V. Toward Reliable Density Functional Methods without Adjustable Parameters: the PBE0Model. *J. Chem. Phys.* **1999**, *110*, 6158−6170.

(29) Spackman, M. A. Potential Derived Charges using a Geodesic Point Selection Scheme. *J. Comput. Chem.* **1996**, *17*, 1−18.

(30) Bader, R. F. W. *Atoms in Molecules*; Oxford University Press: Oxford, U.K., 1990.

(31) Lode, P.; Popelier, P. L. A. The QTAIM Perspective of Chemical Bonding. In *The Chemical Bond, Fundamental Aspects of Chemical Bonding*; Frenking, G., Shaik, S., Eds.; Wiley-VCH: Weinheim, Germany, 2014; 271−308.

(32) Gatti, C.; Saunders, V. R.; Roetti, C. Crystal Field Effects on the Topological Properties of the Electron Density in Molecular Crystals: the Case of Urea. *J. Chem. Phys.* **1994**, *101*, 10686−10696.

(33) Regarding the theory and method of this approach see, for example, Scherer, W.; Fischer, A.; Eickerling, G. The Experimental Density Perspective of Chemical Bonding. In *The Chemical Bond, Fundamental Aspects of Chemical Bonding*; Frenking, G., Shaik, S., Eds.; Wiley-VCH: Weinheim, Germany, 2014; pp 309−344.